Electronic Supplementary Information

Fibril-induced neurodegenerative disorders in Aβ-mutant Drosophila model: therapeutic targeting using ammonium molybdate

Sudipa Manna,[a,†] Puja Karmakar,[b] Bikash Kisan,[b] Monalisa Mishra,*[b] Nilotpal Barooah,[a] Achikanath C. Bhasikuttan*[a,c] and Jyotirmayee Mohanty*[a,c]

[a]Radiation & Photochemistry Division, Bhabha Atomic Research Centre, Mumbai, 400085 INDIA. [b]Department of Life Science, National Institute of Technology Rourkela, Odisha 769008, INDIA. [c]Homi Bhabha National Institute, Training School Complex, Anushaktinagar, Mumbai, 400094, India. [†]Present address: Analytical Chemistry Division, Bhabha Atomic Research Centre, Mumbai, 400085 INDIA.

Experimental

Human insulin was obtained from Sigma-Aldrich and was used as received. Ammonium heptamolybdate was purchased from Sisco Research Laboratories Pvt. Ltd., India and used without further purification. Thioflavin T (ThT) obtained from Sigma-Aldrich was purified by column chromatography on a silica gel column with mildly acidic methanol (1 mL of 1 N HCl in 500 mL of methanol) as eluent. The purity was further confirmed by the ^{1}H NMR, which showed only the corresponding peaks as reported for ThT.[1] Nanopure water (Millipore Gradiant A10 System; conductivity of 0.06 μS cm^{-1}) was used throughout for solution preparation. Wild type *Oregon-R Drosophila melanogaster* and *UAS-eye Gal4-Aβ 42/ CyO+* flies used in this study were obtained from the C-CAMP Fly Facility, Bangalore and BHU, India, respectively. Standard Fly foods (Sucrose, corn meal, yeast, type 1 agar, nipagin and propionic acid) were procured from HiMedia.

The sample solution was prepared by dissolving human insulin (1.5mg/ml) in 25 mM of HCl, 100 mM NaCl (pH ~1.7) and ~10 μM ThT was added to this solution, as reported in the literature.[2] The net solution was incubated at 60°C. For the fibril inhibition, ammonium molybdate was added to the insulin solution before incubation. Initially a white turbid solution was obtained upon addition of ammonium molybdate which becomes clear after incubation for 30 minutes at 60°C. Small aliquots (~200μL) of samples were drawn at regular time intervals, diluted judiciously with blank solvent and fibril formation was monitored by recording the absorption, fluorescence spectra and fluorescence decay traces of the sample solution.

Spectroscopic measurements. Absorption spectra were recorded using UV-VIS-NIR spectrophotometer (UV-3600 Plus, Shimadzu, Japan). Steady-state fluorescence spectra were recorded using a FS5 spectrofluorometer (Edinburgh Instruments, UK). For steady state fluorescence

measurements, the samples were excited at 390 nm. The spectra were measured in the wavelength range 200−700 nm using a quartz cuvette with 1.0 cm path length. Fluorescence lifetime measurements were carried out using a time-correlated-single photon-counting (TCSPC) spectrometer (IBH, UK). In the present work, a 374 nm diode laser (~100 ps, 1 MHz repetition rate) was used for excitation and a PMT was used for fluorescence detection. From the measured decay traces, the time constants were evaluated following a reconvolution procedure.[3] The fluorescence decays, I(t) were analyzed using a multi-exponential function as

$$I(t) = \sum B_i \exp(-t / \tau_i) \quad (1)$$

where, B_i and τ_i are the pre-exponential factor and fluorescence lifetime for the i^{th} component, respectively. Reduced chi-square (χ^2) values and random distribution of the weighted residuals among data channels were used to judge the acceptance of the fits.

The dynamic light scattering (DLS) measurements were carried out using Malvern 4800 Autosizer employing an Ar ion laser (λ=514.5 nm) and digital correlator. The scattered light intensity was monitored at a scattering angle of 130° and the intensity correlation function over a time range of 10^{-6} to 1 s was computed. Zeta potentials were determined with a Nanosizer Z (Malvern Instruments, Malvern, UK) by phase analysis light scattering. The light source was He-Ne laser operated at 633 nm operating at 4 mW. The zeta potential (ζ) values were calculated from the electrophoretic mobility data using Smoluchowsky approximation. The experiment was carried out using a quartz cuvette (universal 'dip' cell) with 10 mm light pathway.

CD measurements were performed using MOS-500 spectropolarimeter from BioLogic, France. The CD spectra were recorded in quartz cuvettes of 1cm path length with Insulin (2µM) followed by the successive addition of ammonium molybdate solution at pH2. FTIR measurements were performed using Bruker ALPHA II FT-IR spectrometer in diffuse reflectance mode.

ITC experiments were carried out using a Microcal iTC 200 from Malvern, UK. 20 µM of ammonium molybdate solution in the sample cell was titrated by adding consecutively 19 injections of 2µl of 1 mM of insulin at pH 2 and 25 °C. The first data point was removed from the data set prior to curve fitting with Origin 7.0 software. Thermodynamic parameters of the complex formation were also evaluated using the estimated binding constant value and molar reaction enthalpy (ΔH).

Fly stock maintenance. The food media used for rearing the *Oregon-R*and *UAS-eye Gal4-Aβ 42/ CyO+*flies were composed of corn meal, sucrose, and agar-agar (type-1). To prevent any type of fungal and mould contamination Propionic acid and Nipagin were added to the food.

The flies were maintained at 25°C temperature, 60% relative humidity and they were exposed to a normal day-night life cycle. All the experiments were replicated in triplicate. *Oregon R* flies were treated with molybdate solutions in two different ways.

Fly set up 1. Flies were transferred to the 10µM+2% oil, 20 µM+2% oil and 40 µM +2% oil $Mo_7O_{24}^{6-}$ treated vials to check the combined effect of high fat diet and various concentration $Mo_7O_{24}^{6-}$ on fly development.

Fly set up 2. Control flies were fed with standard fly food having 2% coconut oil. 48 hours' pupae were collected from the vial and transferred to three different concentrations of 10µM, 20µM, 40µM of $Mo_7O_{24}^{6-}$. Once the adults will hatch, they eat various concentrations of $Mo_7O_{24}^{6-}$ treated food.

Mutant fly set up. Flies were collected from the stock of *UAS-eye Gal4-Aβ 42/ CyO+* and they were transferred to the food vials containing 10µM, 20µM, 40µM of $Mo_7O_{24}^{6-}$ treatment.

2.4. Larval crawling assay for set up 1 and set up 2. Larvae crawling assay provides the information about the crawling path of the larvae. For this experiment 3rd inster larvae were collected from the food vial and washed with 1X PBS to remove the food ingredient from the outer surface. Next, the larvae were allowed to crawl for 1 min in a 90 mm petri plate having 2% solidified agarose gel in it. The path of the larvae was traced and from the recorded path the velocity of the larvae per minute was determined. The distance travelled by the larvae was plotted in a graph. The crawling path of the larvae treated with 10µM molybdate along with 2% oil and 20 µM molybdate + 2% oil shows a defective crawling path suggesting damage in motor neurons.[4-7] The crawling path becomes normal at 40µM molybdate along with 2% oil treated group. A significant increase in crawling speed was observed in 20µM molybdate + oil and 40µM molybdate + oil treated larvae (Fig. S7).

Climbing assay for various set ups. Climbing assay is a simple behavioral test used to detect the locomotory defect.[4, 8] For this assay, 30 flies from the 1st generation set up 1 were anesthetized to check the climbing behaviour.[9] From set up 2, after seven days of eating of various concentrations of $Mo_7O_{24}^{6-}$, flies were subjected to climb. The flies were transferred to a 100 ml measuring cylinder. A mark was made at 80 ml of the cylinder which measured approximately 16 cm. The mouth of the measuring cylinder was closed with a cotton plug to avoid the escape of the flies. Adult flies were transferred to the measuring cylinder and allowed to acclimatize to the new environment. Before starting the assay, the flies were brought down to the bottom of the measuring cylinder by gently tapping the cylinder against a hard surface three to four times. The climbing of the flies was recorded for 10 s and the number of flies that crossed the 80 ml mark was counted. The experiment was repeated for at least six times.

Adult phenotype checks. Flies hatched from various treatment groups were subjected to check the phenotypic defects. For these 50 flies were removed from each vial and anesthetized with ethyl ether and screened under a stereomicroscope. This was repeated from three different independent set ups.

In case of mutants, Aβ42-mutant flies of different $Mo_7O_{24}^{6-}$ treatment groups were collected and their eye phenotypes were screened under a digital camera (500X magnification USB Digital Microscope Portable Lab Video Camera Magnifier). The defects were measured and compared with the non-treated Aβ42-mutant flies. Images were also recorded using an Environmental scanning electron microscope (ESEM; FEI Quanta FEG 250).

ThioflavinT (ThT) staining of adult mutant brain and eye. Whole brain and of $Mo_7O_{24}^{6-}$ treated Aβ-mutant adult flies were used to stain the Aβ42 fibril deposits.[10] This analysis was performed to check the ability of the $Mo_7O_{24}^{6-}$ to break the Aβ42 fibril in mutant flies. The number of bright spots was measured to quantify the presence of the Aβ42 fibril deposits in the brain and eye of treated flies. The images were compared with control mutants which were not treated with $Mo_7O_{24}^{6-}$.

For this adult fly brains and eyes of mutant flies treated with $Mo_7O_{24}^{6-}$ were dissected out and stored in 4% Paraformaldehyde (Himedia) and permeabalized with 100% DMSO (Himedia) for 5 minutes and in 4% BSA (Himedia) + Twin20 (Sigma) for whole night in 4°C refrigerator. The samples were stained with 0.5% ThT for one night and destained with 50% ethanol for 15 minutes with 2 wash next day. Samples were washed in PBS for three times and were mounted in 20% Glycerol (Himedia). Slides were observed under a confocal microscope (Leica TCS SP8, CLSM).

Statistical analysis. The experiments were repeated for three times for all the concentrations and with same number and age of flies. Graph Pad Prism 5.0 software was used to plot the graphs. All the analysis was performed using two-tailed unpaired Student's t-test with confidential intervals of 95%. All the data were represented in Mean ± SEM value. $p < 0.5$ value was considered as significant.

Note S1: CD measurements

Human insulin displays a characteristic negative CD band with peaks at ~210 nm and ~222 nm in the Far-UV region due to the absorption of amide bonds (Fig. S1, trace 1). Upon incremental additions of molybdate, there was slight changes in the intensity of both the negative peaks, however, a broad CD band in the near-UV region range (250 nm to 350 nm) with an approximate peak at ~295 nm appeared. The intensity of this broad band increased and attained saturation at ~32 μM of molybdate. Based on the available literature data, we attribute this change in the CD spectrum due to the interaction of Insulin with the molybdate. It has been reported that the aromatic residues such as tyrosine and phenylalanine and cysteine do not have an intrinsic CD signal due to the planarity of their rings. However, a change in the planarity of the rings due to the interaction and/or assembly formation

induces chirality in the aromatic residues which would result in to the observed near-UV CD band in insulin-molybdate system.[11]

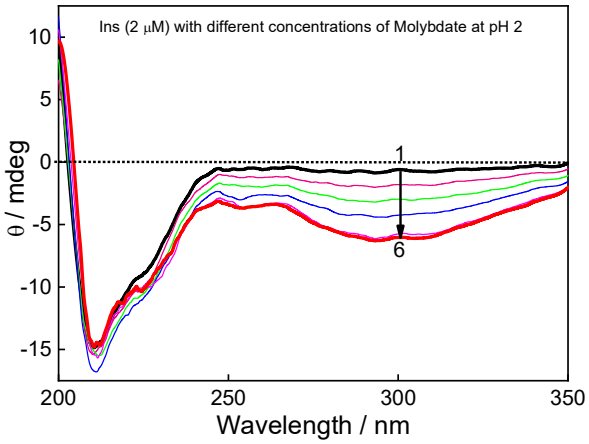

Fig. S1 CD spectra of insulin (2μM) at different concentrations of ammonium molybdate at pH 2. $[(NH_4)_4(Mo_8O_{26})]$/μM: 0 (1), 2 (1), 4 (3), 8 (4), 24 (5) and 32 (6).

Note S2: FTIR spectral measurements

Upon titration of Insulin with molybdate at pH 2, with increasing concentration of molybdate the solution turned turbid indicating interaction among them and the formation of less soluble assembly. The precipitate of Ins-molybdate assembly was separated by Freeze-dryer and the FTIR spectrum of this assembly has been recorded along with their individual components (Fig. S2). Insulin displays two characteristic signals at ~1647 cm^{-1} and ~1531 cm^{-1} corresponding to C=O stretching vibrations present in respective amide I and amide II bands. In case of Ins-molybdate assembly these bands displayed ~3-4 cm^{-1} shifts towards the higher frequency. Furthermore, it was observed in the Ins-molybdate assembly that the characteristic Mo-O stretching vibration appeared at 620 cm^{-1} and the Mo−O−Mo stretching vibration mode at 870cm^{-1} and Mo=O stretching vibration at 914cm^{-1} of molybdate anion (Fig. S2). The vibration modes at 870cm^{-1} and 914cm^{-1} displayed significant shift to high frequency region, 910 cm^{-1} and 947 cm^{-1}, respectively, indicating a strong interaction/complex formation between molybdate and Insulin.[12,13] The strong asymmetric bending vibration of the NH_4^+ counter ion at 1400 $cm^{-1,}$ which was observed in the molybdate only spectrum disappeared in the Ins-molybdate assembly probably due to its exchange with the cationic insulin residues. These experimental observations confirm strong interaction of insulin with ammonium molybdate leading to the formation of Ins-molybdate assembly under our experimental conditions.

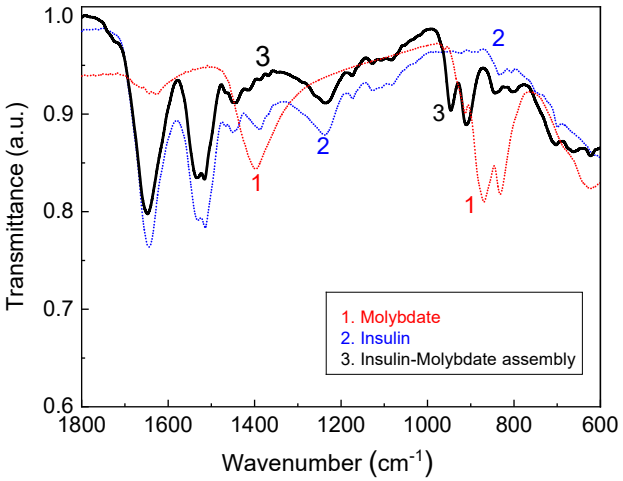

Fig. S2 FTIR spectra of molybdate (1), insulin (2) and insulin:molybdate assembly (3).

Note S3: ITC measurement

To substantiate and evaluate the thermodynamic parameters of the interaction of ammonium molybdate with insulin, ITC titrations were performed at pH 2. Figure S3 shows the ITC profile of the titration of insulin with ammonium molybdate after correction of heat of dilution in aqueous medium. Due to the presence of many protonated amino acid residues in insulin, electrostatic interaction of more than one molybdate anion with the protein may be anticipated. The ITC profile displayed an endothermic progression with consecutive addition of ammonium molybadate for which a data fitting adopting sequential 1:3 binding model led to a rough estimation of binding constants in the order of 10^4-10^6 M^{-1}. It was further observed that the estimated ΔG based on the ΔH and ΔS values to be negative confirming thermodynamically favorable binding of ammonium molybdate with insulin protein under the experimental conditions and the ΔG values are given below.

ΔH_1 = 6.5 kcal mol^{-1}, $-T\Delta S_1$ = -13.9 kcal mol^{-1}, ΔG_1 = -7.4 kcal mol^{-1}; ΔH_2 = -15.34 kcal mol^{-1}, $-T\Delta S_2$ = 9.0 kcal mol^{-1}, ΔG_2 = -6.3 kcal mol^{-1} and ΔH_3 = 12.5 kcal mol^{-1}, $-T\Delta S_3$ = -21.3 kcal mol^{-1}, ΔG_3 = -8.8 kcal mol^{-1} for Insulin:molybdate complex.

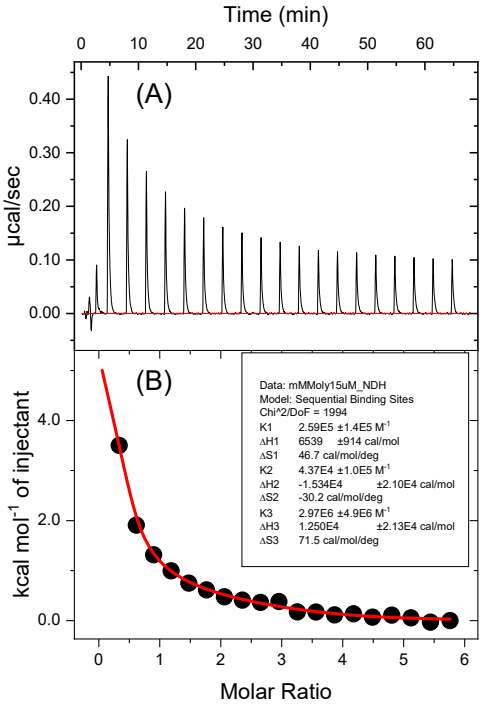

Fig. S3 (A) Raw data for the titration of 20 µM ammonium molybdate with 1 mM insulin at pH 2 and 25 °C, showing the calorimetric response as successive injections of insulin are added to the sample cell. (B) Integrated heat profile of the calorimetric titration shown in panel A. The solid line represents the best nonlinear least-squares fit to a sequential 1:3 binding-site model.

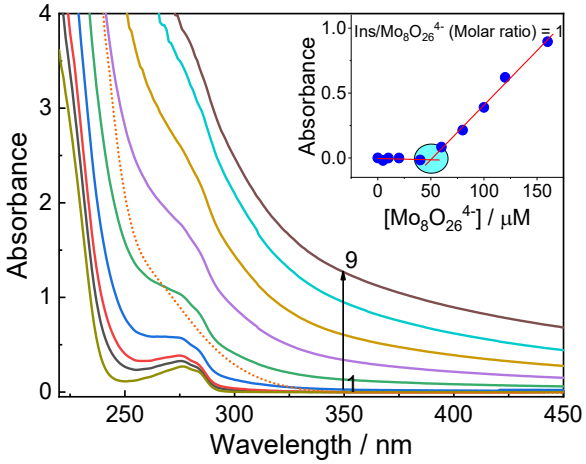

Fig. S4 Absorption spectra of insulin at different concentrations of ($Mo_8O_{26}^{4-}$) at pH ~2. [$Mo_8O_{26}^{4-}$] /µM: 0 (1), 10 (2), 20 (3), 40 (4), 60 (5), 80 (6), 100 (7), 120 (8) and 160 (9). Inset shows the absorbance at 350 nm of insulin at different concentrations of ($Mo_8O_{26}^{4-}$). Dotted line shows the absorption spectra of 160 µM ($Mo_8O_{26}^{4-}$).

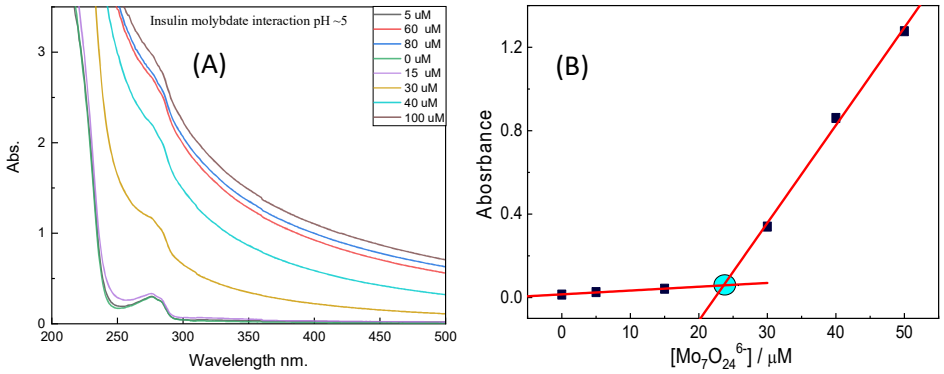

Fig. S5 Absorption spectra (A) and absorbance at 350 nm (B) of insulin at different concentrations of ($Mo_7O_{24}^{6-}$) at pH 5-6. [$Mo_7O_{24}^{6-}$]/µM: 0 (1), 5 (2), 15 (3), 30 (4), 40 (5), 60 (6), 80 (7) and 100 (8).

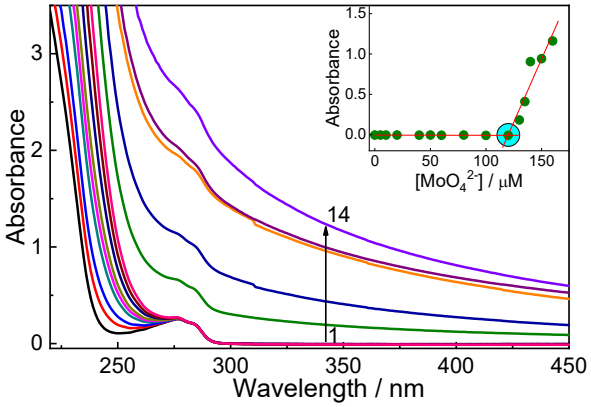

Fig. S6 Absorption spectra of insulin at different concentrations of (MoO_4^{2-}) at pH 7.4. [MoO_4^{2-}]/µM: 0 (1), 10 (2), 20 (3), 40 (4), 50 (5), 60 (6), 80 (7), 100 (8), 120 (9), 130 (10), 135 (11), 140 (12), 150 (13) and 160 (14). Inset shows the absorbance at 350 nm of insulin at different concentrations of (MoO_4^{2-}).

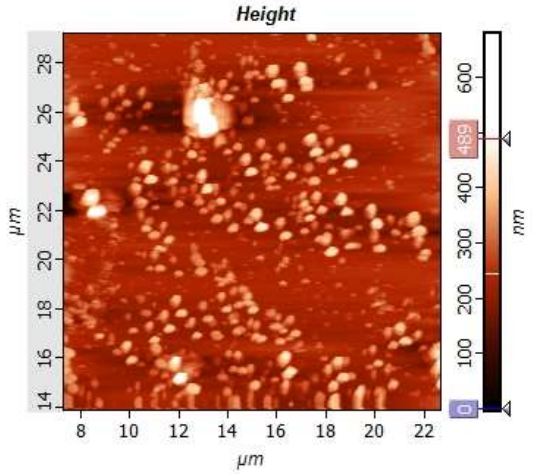

Fig. S7 AFM images of insulin (250 µM) with molybdate (100 µM) at pH 2.

Table S1. Particle size measurements of insulin assembly at different concentrations of $Mo_7O_{24}^{6-}$ at pH 5-6 using DLS.

$[Mo_7O_{24}^{6-}]$ (μM)	Average particle size (nm)
0	263
5	446
10	618
20	804
40	965
60	1205
100	1553
160	1842
250	2013

Table S2. Lifetime of ThT dye with different concentrations of $[Mo_8O_{26}^{4-}]$. λ_{ex} = 374 nm, λ_{mon} = 490 nm.

$[Mo_8O_{26}^{4-}]$ (μM)	**τ_1 (%) ns**	**τ_2 (%) ns**	**τ_{avg} (ns)**
0	1.64 (11)	2.42 (89)	2.33
5	1.16 (13)	2.33 (87)	2.18
10	1.13 (21)	2.29 (79)	2.05
20	0.83 (31)	2.11 (69)	1.71
30	0.69 (39)	2.00 (61)	1.49
40	0.64 (38)	1.97 (62)	1.46
60	0.58 (40)	1.94 (60)	1.40
100	0.54 (41)	1.89 (59)	1.34
300	0.56 (43)	1.91 (57)	1.33

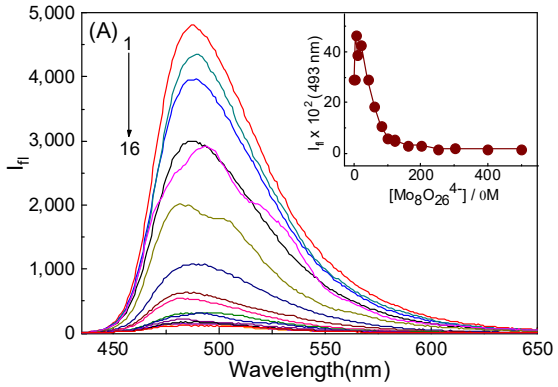

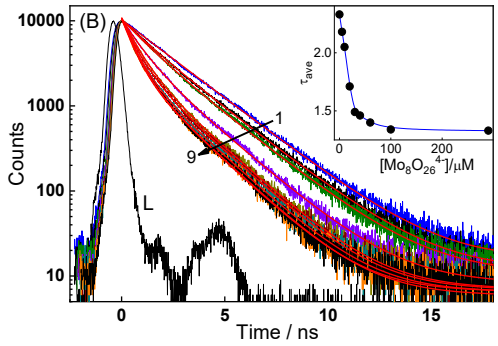

Fig. S8 (A) Fluorescence spectra and (B) lifetime decay traces of ThT during fibril disintegration at pH 2 with different concentrations of ($Mo_8O_{26}^{4-}$), 250 μM insulin was used to synthesize fibrils. (A) [$Mo_8O_{26}^{4-}$] / μM: 0 (1), 5 (2), 10 (3), 20 (4), 40 (5), 60 (6), 80 (7), 100 (8), 120 (9), 160 (10), 200 (11), 250 (12), 300 (13), 400 (14), 500 (15) and 1000 (16). (B) [$Mo_8O_{26}^{4-}$] / μM: 0 (1), 5 (2), 10 (3), 20 (4), 30 (5), 40 (6), 60 (7), 100 (8) and 300 (9). L represents the lamp profile. λ_{ex} = 374 nm and λ_{mon} = 490 nm.

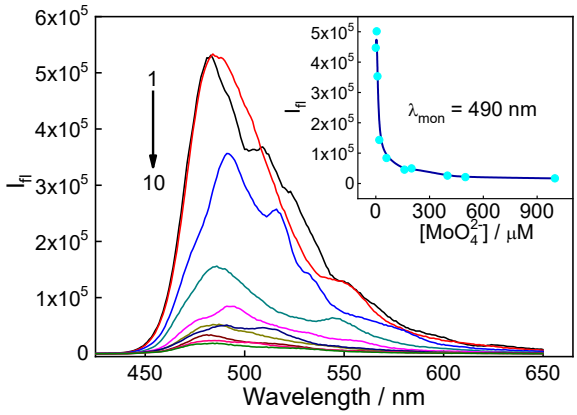

Fig. S9 Fluorescence spectra of ThT during fibril disintegration at pH 7.4 with different concentrations of (MoO_4^{2-}), 250 μM insulin was used to synthesize fibrils. [MoO_4^{2-}] / μM: 0 (1), 5 (2), 10 (3), 20 (4), 60 (5), 160 (6), 200 (7), 400 (8), 500 (9) and 1000 (10).

Table S3. Particle size of fibrils with different concentrations of ammonium molybdate at pH 5-6.

[$Mo_7O_{24}^{6-}$](μM)	**Average particle size (nm)**
10	2139
50	1956
150	1653
750	1570
1000	1313
1250	1069

Table S4. Changes in the Zeta potential values of fibril with the addition of ammonium molybdate at pH 2 and pH 5-6.

$[Mo_8O_{26}^{4-}]$ (μM)	Zeta potential (mV) at pH 2	$[Mo_7O_{24}^{6-}]$ (μM)	Zeta potential (mV) at pH 5-6
0	24.9	0	11.33
20	23.1	10	3.34
150	10.93	20	-4.94
250	2.94	--	--
300	-0.20	--	--

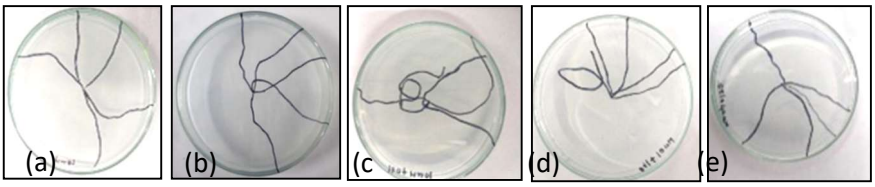

Fig. S10 Crawling path of larvae without any treatment (a), larvae treated with 2% coconut oil (b), b with 10 μM (c), 20 μM (d) and 40 μM (e)of $Mo_7O_{24}^{6-}$. Crawling path of larvae with and without treatment of 40 μM $Mo_7O_{24}^{6-}$ + 2% oil remains almost similar.

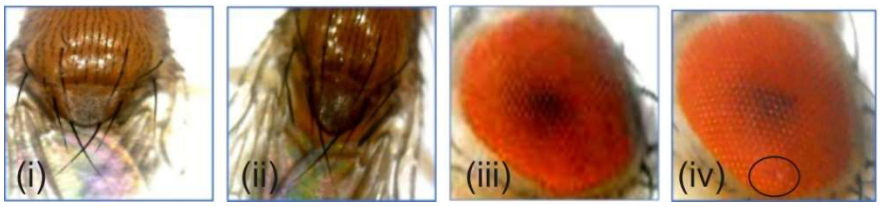

Fig. S11 Eye and thorax defect in the flies treated with oil and $Mo_7O_{24}^{6-}$ (i and iii) normal fly feed with 2% oil, (ii) normal fly feed with 2% oil and 10 μM $Mo_7O_{24}^{6-}$ and (iv) normal fly feed with 2% oil and 20 μM $Mo_7O_{24}^{6-}$.

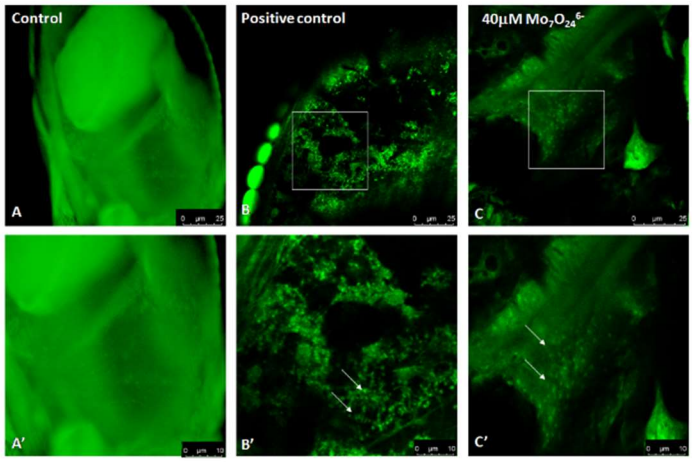

Fig. S12 Confocal microscopic images of the adult eyes of control (A and A': normal fly), Aβ mutant flies (B and B': positive control) and $Mo_7O_{24}^{6-}$ (40 μM) treated Aβ mutant fly (C and C'). A', B' and C' are the enlarged images of A, B, and C, respectively

References

1 S. Dutta Choudhury, J. Mohanty, H. P. Upadhyaya, H. Pal, *J. Phys. Chem. B* **2009**, *113*, 1891.

2 J. Mohanty, S. Dutta Choudhury, H. Pal, A. C. Bhasikuttan, *Chem. Commun*. **2012**, *48,* 2403.

3 J. R. Lakowicz, *Principles of fluorescence spectroscopy*; Springer: New York, **2006.**

4 A. Gautam, C. Gautam, M. Mishra, V. K. Mishra, A. Hussain, S. Sahu, R. Nanda, B. Kisan, S. Biradar, R. K. Gautam, *RSC Adv*. **2019**, *9*, 40977.

5 C. D. Nichols, J. Becnel, U. B. Pandey, *J. Vis. Exp*. **2012**, *61*, e3795.

6 S. Priyadarsini, S. K. Sahoo, S. Sahu, S. Mukherjee, G. Hota, M. Mishra, *Environ. Sci. Pollut. Res*. **2019**, *26*, 9560.

7 D. Sabat, A. Patnaik, B. Ekka, P. Dash, M. Mishra, *Physiol. Behav.* **2016**,*167*, 76.

8 P. K. Mishra, A. Ekielski, S. Mukherjee, S. Sahu, S. Chowdhury, M. Mishra, S. Talegaonkar, L. Siddiqui, H. Mishra, *Biomolecules* **2019**, *9*, 363.

9 S. T. Madabattula, J. C. Strautman A. M. Bysice, J. A. O'Sullivan, A. Androschuk, C. Rosenfelt, K. Doucet, G. Rouleau, F. Bolduc, *J. Vis. Exp*. **2015**, *100*, e52741.

10 H.-C. Chiang, L. Wang, Z. Xied, A. Yaua, Y. Zhong, *Proc. Natl. Acad. Sci. USA* **2010**, *107*, 7060.

11 M. F. Pignataro, M. G. Herrera, V. I. Dodero, *Molecules* **2020**, *25*, 4854.

12 H. Oudghiri-Hassani, S. Rakass, M. Abboudi, A. Mohmoud, F. Al Wadaani, *Molecules* **2018**, *23*, 1462.

13 S. Sadighi, S. K. M. Targhi, *Bull. Chem. React. Eng. Catal.* **2017**, 12, 52.